General Disclaimer

One or more of the Following Statements may affect this Document

- This document has been reproduced from the best copy furnished by the organizational source. It is being released in the interest of making available as much information as possible.

- This document may contain data, which exceeds the sheet parameters. It was furnished in this condition by the organizational source and is the best copy available.

- This document may contain tone-on-tone or color graphs, charts and/or pictures, which have been reproduced in black and white.

- This document is paginated as submitted by the original source.

- Portions of this document are not fully legible due to the historical nature of some of the material. However, it is the best reproduction available from the original submission.

X-643-69-503

PREPRINT

NASA TM X-63742

RESPONSE OF ORBIT DETERMINATION SYSTEMS TO MODEL ERRORS

R. K. SQUIRES
D. S. WOOLSTON
H. WOLF

NOVEMBER 1969

GSFC

GODDARD SPACE FLIGHT CENTER

GREENBELT, MARYLAND

RESPONSE OF ORBIT DETERMINATION SYSTEMS TO MODEL ERRORS

R. K. Squires
D. S. Woolston
Special Projects Branch

and

H. Wolf
Analytical Mechanics Associates, Inc.
Jericho, New York

November 1969

GODDARD SPACE FLIGHT CENTER
Greenbelt, Maryland

RESPONSE OF ORBIT DETERMINATION SYSTEMS TO MODEL ERRORS

By

R. K. Squires
D. S. Woolston
Special Projects Branch
Goddard Space Flight Center
Greenbelt, Maryland

and

H. Wolf
Analytical Mechanics Associates, Inc.
Jericho, New York

Abstract

This paper discusses the response of a sequential and a Bayes minimum variance orbit determination system to errors in the force model. For the most part, the error is introduced into the central mass. In most instances the processors do not know of nor solve for the error. A half orbit of generated data at one minute intervals is used in all cases.

It is shown that they both arrive at the same orbit even after the so-called "divergence" of the sequential processor.

It is further shown that the residual patterns obtained in the final orbit contain frequencies which appear like the 6th order zonal harmonic even though the error was due to the zeroth order term. Therefore it may be fallacious to analyze the frequency content of residuals.

Finally, when this philosophy is applied in a manner similar to the "mascon" reduction technique, a residual pattern is obtained which bears a striking resemblance to the lunar orbiter residual patterns although in fact no such "mascons" exist in the process. Hence, the technique of deriving "mascons" from a differentiation of residual patterns is suspect.

RESPONSE OF ORBIT DETERMINATION SYSTEMS TO MODEL ERRORS

INTRODUCTION

There are two fundamentally different orbit determination systems, namely, least squares or batch processing and sequential, usually Kalman processing. It is well known that under ideal conditions i.e. if all the assumptions made in their derivations are met; they converge to the same solution. In orbit determination, this means they find the same trajectory.

Least squares has been in use for generations and is currently the most accepted for scientific analysis. Sequential processing has only recently been introduced and has seen only limited use on practical problems.

The mathematical development of both methods has been widely published and will not therefore be repeated here. Occasionally the equations will be used for the purpose of clarifying the discussion.

Applying either of these techniques to orbit determination is a very complex task which, in general, tends to mask, if not obliterate the physical picture of what is taking place. Often they have been used without rigor i.e. in violation of one or more of the assumptions made in their derivation. It is no wonder that strange results occur. There exists a vast amount of literature on how these systems respond in the ideal, theoretical world but little exists which demonstrates how they respond to things approaching the real world. This is partly because in the real world the true or actual orbit is never known. At best then, one can attempt to simulate certain features of the real

world and test the system responses under controlled conditions. This work represents at least an initial step in this direction.

Two computer programs are used in this study, which are identical in every respect except in the statistical subroutine. One uses a Bayes batch processor, the other the Kalman sequential processor. In the latter, the capability exists to first scan the data to examine residual patterns before the differential correction pass and again to scan after the differential correction pass.

In this study ideal observations were generated for a single half orbit of a point mass around the earth. The data are range and range-rate observations made from a single tracking station located at a fixed point in inertial space at about the 24 hour altitude. Data was generated at one minute intervals using the SAO '66 gravitational model. The orbit being tracked had the following initial osculating elements:

Epoch

$a = 2.099$ ER

$e = 0.500$

$i = 100^{\circ}.00$

$\omega = 0^{\circ}.003$

$\Omega = 0^{\circ}.0$

$t_p = 1.289$ hrs.

The pericenter was on the equator and so was the tracking station. The noise added to the ideal data by a random number generator was 5.0 meters in range and about 2.0 mm/sec in range-rate.

DIVERGENCE

The first phenomenon to be discussed is that of the so-called "Divergence" of the sequential processor. In Figure 1, the residuals, i.e. the observed minus computed observations, are shown for a sequential orbit determination pass through the data. In this case, the central mass is in error by one in the fourth significant figure. This large error was selected so that the error was well above the noise. There has been no attempt to solve or account for this error in the statistical computations. A large and arbitrary a priori matrix has been used (Diagonal, cartesian, 1. Km each position coordinate and 1. m/s velocity) and with this low noise data, its influence is insignificant after the first six observations. The upper curve shows the residual pattern when only range data are used and the obvious divergence occurs at about 0.9 hours.

The lower curve shows the behavior when only range-rate data is used with divergence occurring at 1.2 hours. The time of divergence is strictly dependent on the noise level assigned to the data but the fact that they both occur at about 1. hour indicates that there is about the same information content in both observation types.

In Figure 2, the same case is shown but both the observation types are used in the determination. Now divergence begins at 0.2 hours; of course the observation types are assumed independent.

An examination of the orbits at the point where divergence occurs shows it to be the point where the covariance matrix can no longer represent the error, i.e. the model has broken down. This may not be a great surprise but continuing to process the data to 154 minutes did

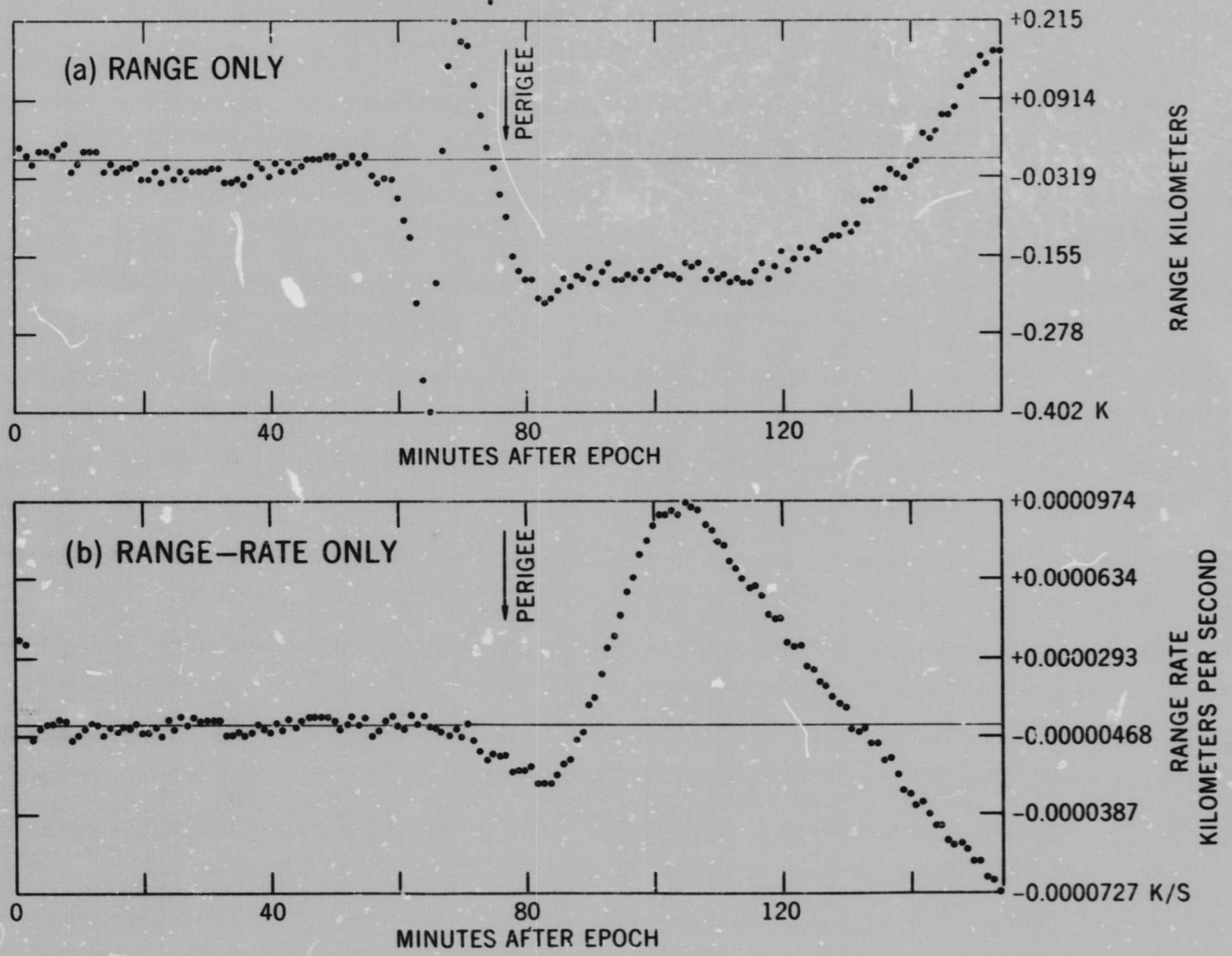
DIVERGENCE
SEQUENTIAL ORBIT DETERMINATION
OBSERVED μ = 19.9094165
COMPUTED μ = 19.9194165
(a) RANGE ONLY
PERIGEE
+0.215
+0.0914
-0.0319
-0.155
-0.278
-0.402 K
RANGE KILOMETERS
0
40
80
120
MINUTES AFTER EPOCH
(b) RANGE–RATE ONLY
PERIGEE
+0.0000974
+0.0000634
+0.0000293
-0.00000468
-0.0000387
-0.0000727 K/S
RANGE RATE
KILOMETERS PER SECOND
0
40
80
120
MINUTES AFTER EPOCH

Figure 1

DIVERGENCE

SEQUENTIAL ORBIT DETERMINATION
RANGE AND RANGE-RATE OBSERVATIONS
OBSERVED $\mu = 19.9094165$
COMPUTED $\mu = 19.9194165$

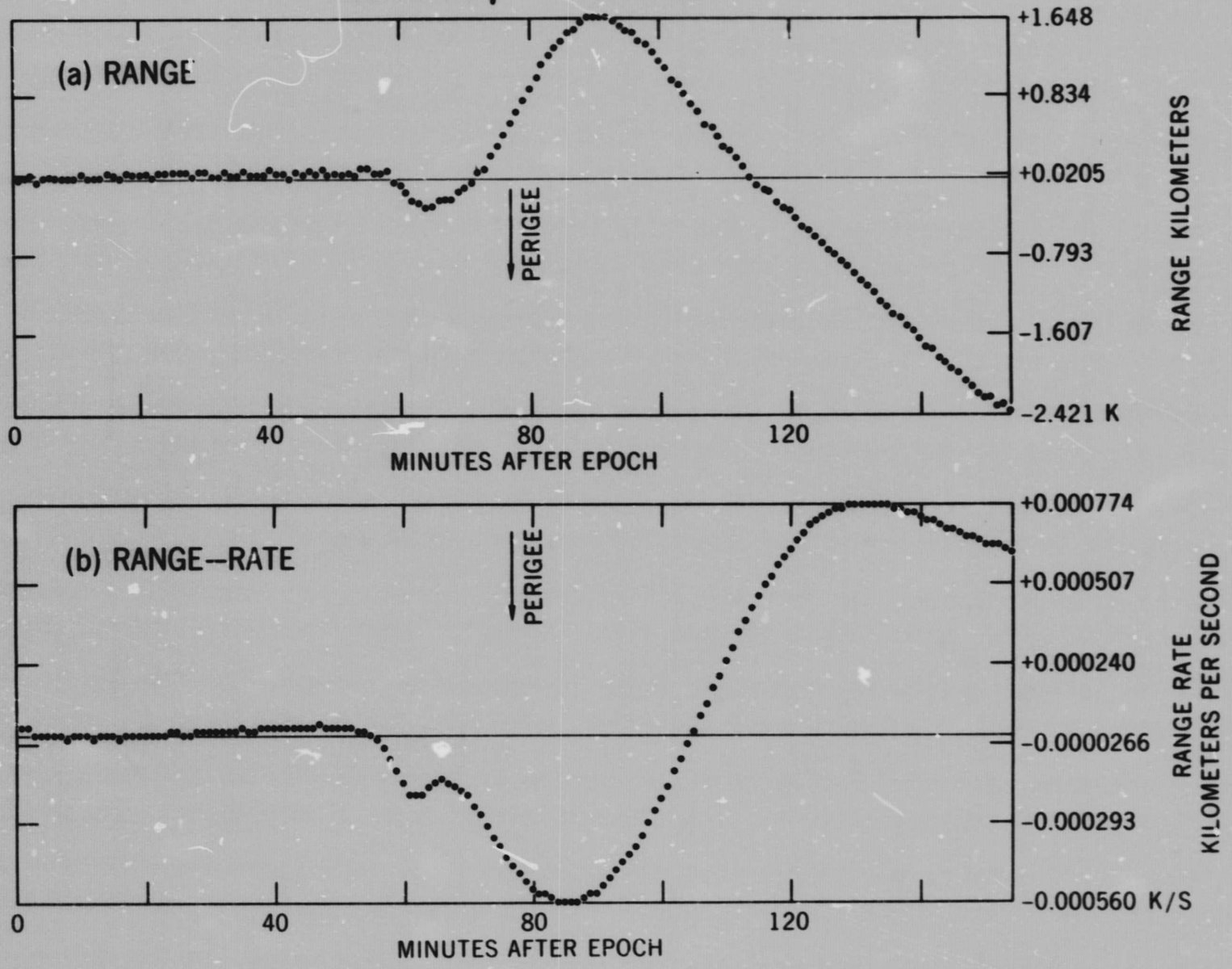

Figure 2

no further damage to the orbit. The covariance matrix, however did get less and less realistic. All three of the cases obtained the same orbit to four significant figures which of course coincides with the model error imposed. The point to emphasize, however, is that divergence tells you not only when your model has failed but in what significant figure the error is occurring.

EQUIVALENCE

The Bayes processor was applied to the same cases and in the next four figures the final scans of both processors are shown, i.e. there is no differential correction being made in these passes. Figure 3 is the case where only range data is used. Obviously, they have both obtained the same orbits. In fact they agree to five or more significant figures. You may note some rather strange residual patterns. These will be discussed later. Figure 4 is the case where range-rate only was used. Figure 5 shows the range residuals when both data types were used in the orbit determination and Figure 6 the range-rate.

A point should be emphasized here that the Bayes does not show an obvious place where the model breaks down. They both, however have matched covariance matrices after convergence has occurred. The Epoch Matrix of the Bayes can be propagated to t-max to compare with the Kalman or the Kalman may be propagated back to Epoch with the same agreement.

BAYES-SEQUENTIAL EQUIVALENCE

RANGE OBSERVATIONS ONLY

OBSERVED $\mu = 19.9094165$

COMPUTED $\mu = 19.9194165$

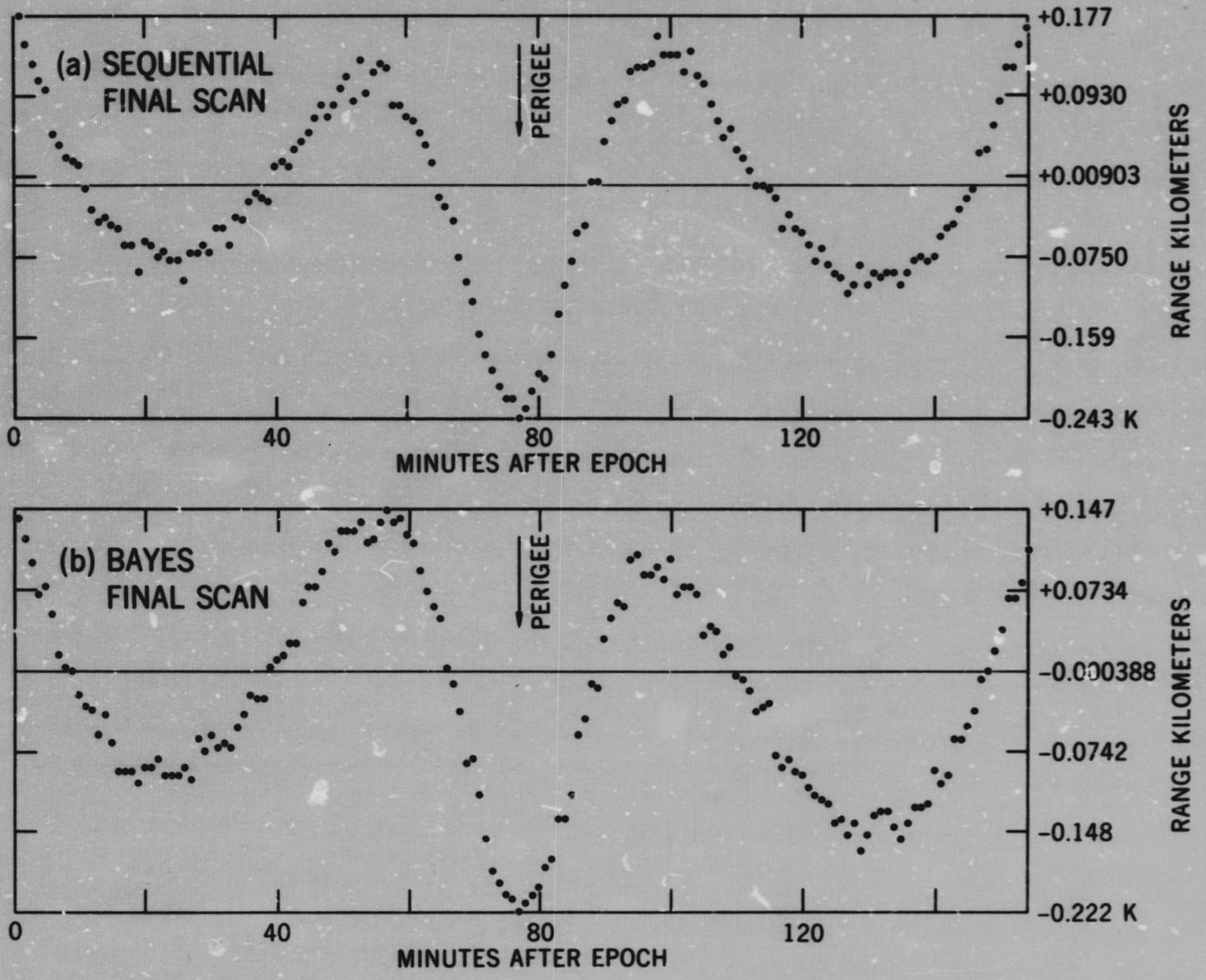

Figure 3

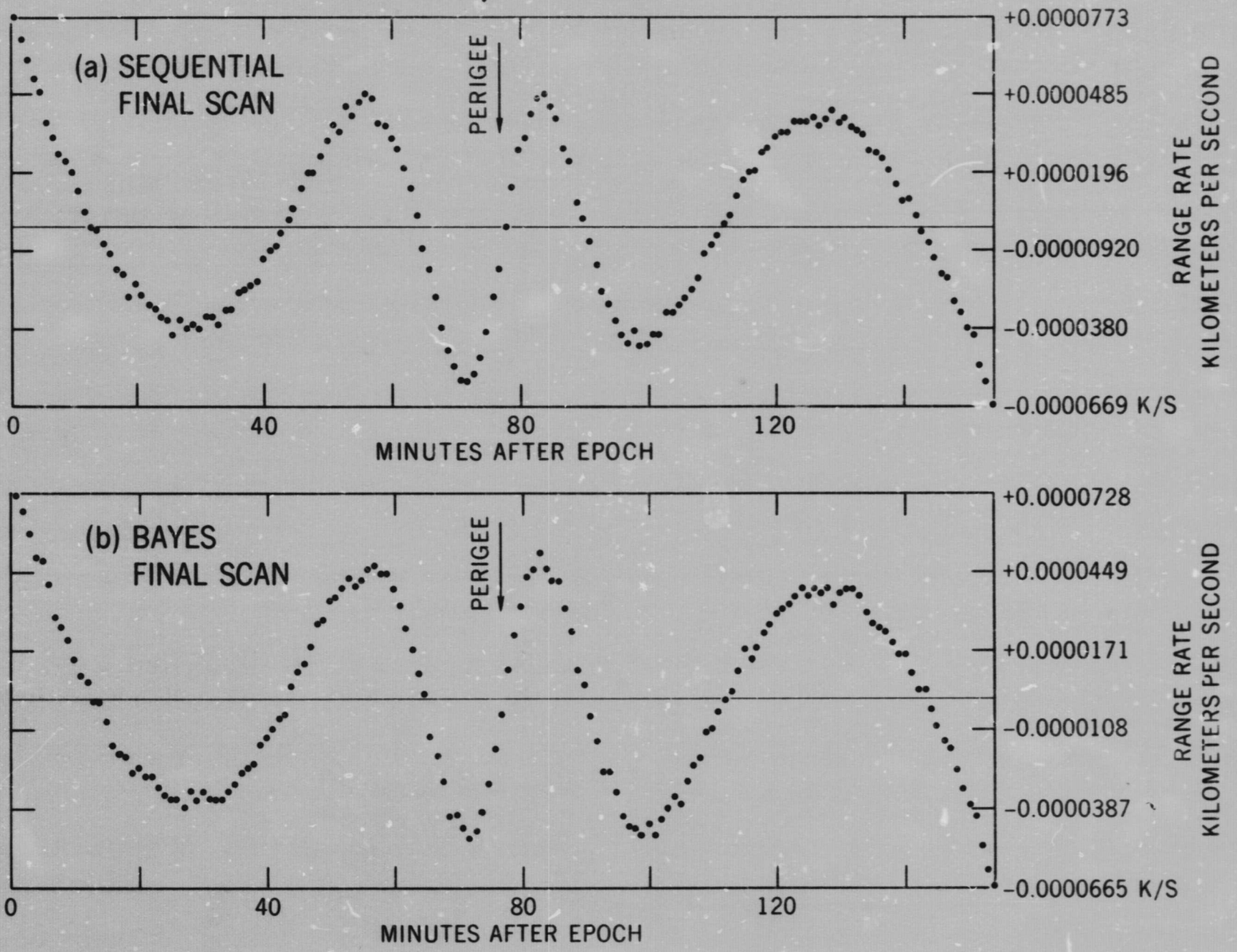
BAYES-SEQUENTIAL EQUIVALENCE
RANGE-RATE OBSERVATIONS ONLY
OBSERVED μ = 19.9094165
COMPUTED μ = 19.9194165
(a) SEQUENTIAL
FINAL SCAN
PERIGEE
+0.0000773
+0.0000485
+0.0000196
-0.00000920
-0.0000380
-0.0000669 K/S
RANGE RATE
KILOMETERS PER SECOND
0
40
80
120
MINUTES AFTER EPOCH
(b) BAYES
FINAL SCAN
PERIGEE
+0.0000728
+0.0000449
+0.0000171
-0.0000108
-0.0000387
-0.0000665 K/S
RANGE RATE
KILOMETERS PER SECOND
0
40
80
120
MINUTES AFTER EPOCH

Figure 4

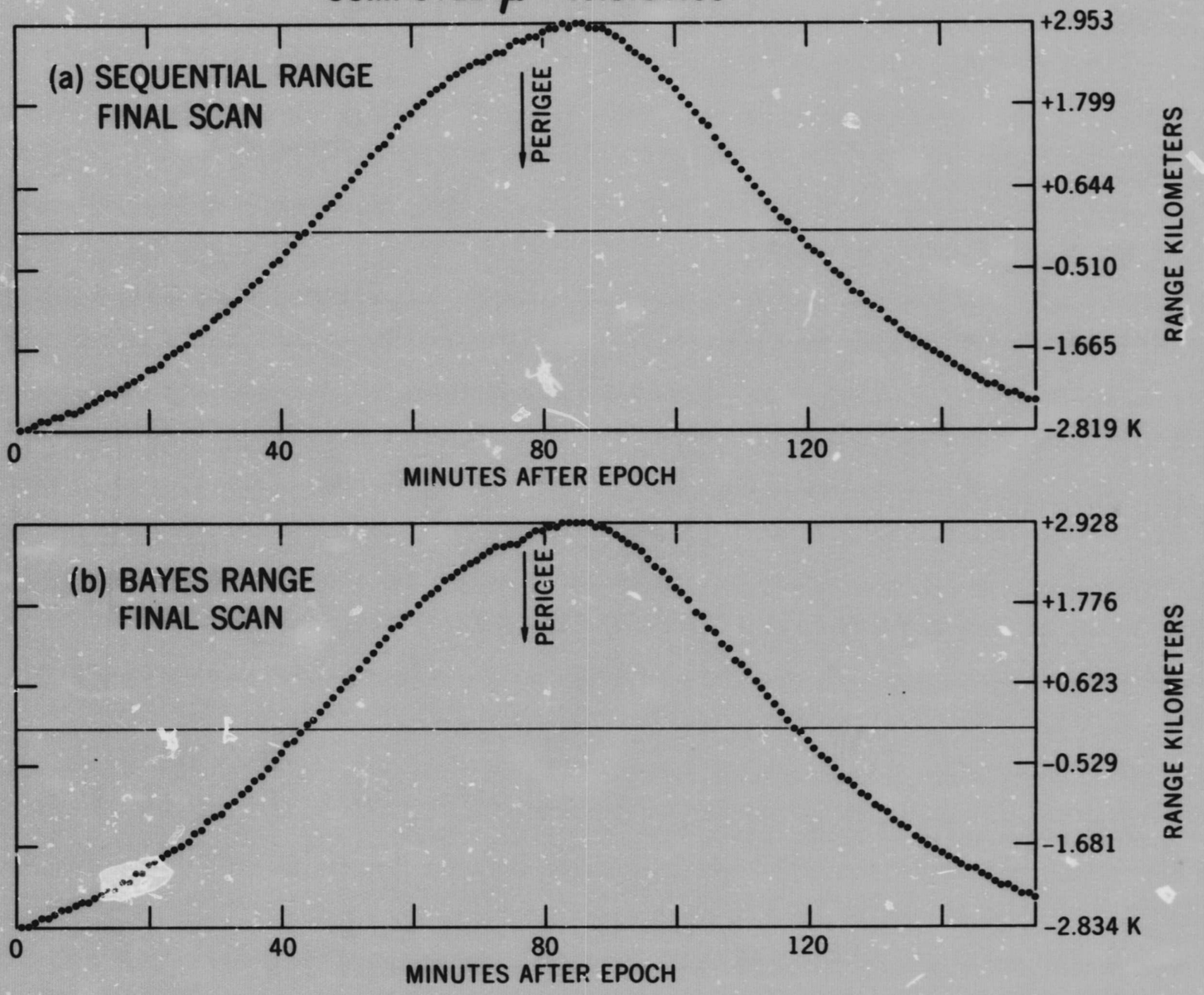
BAYES-SEQUENTIAL EQUIVALENCE
RANGE AND RANGE-RATE OBSERVATIONS
OBSERVED μ = 19.9094165
COMPUTED μ = 19.9194165
(a) SEQUENTIAL RANGE
FINAL SCAN
PERIGEE
+2.953
+1.799
+0.644
-0.510
-1.665
-2.819 K
RANGE KILOMETERS
0
40
80
120
MINUTES AFTER EPOCH
(b) BAYES RANGE
FINAL SCAN
PERIGEE
+2.928
+1.776
+0.623
-0.529
-1.681
-2.834 K
RANGE KILOMETERS
0
40
80
120
MINUTES AFTER EPOCH

Figure 5

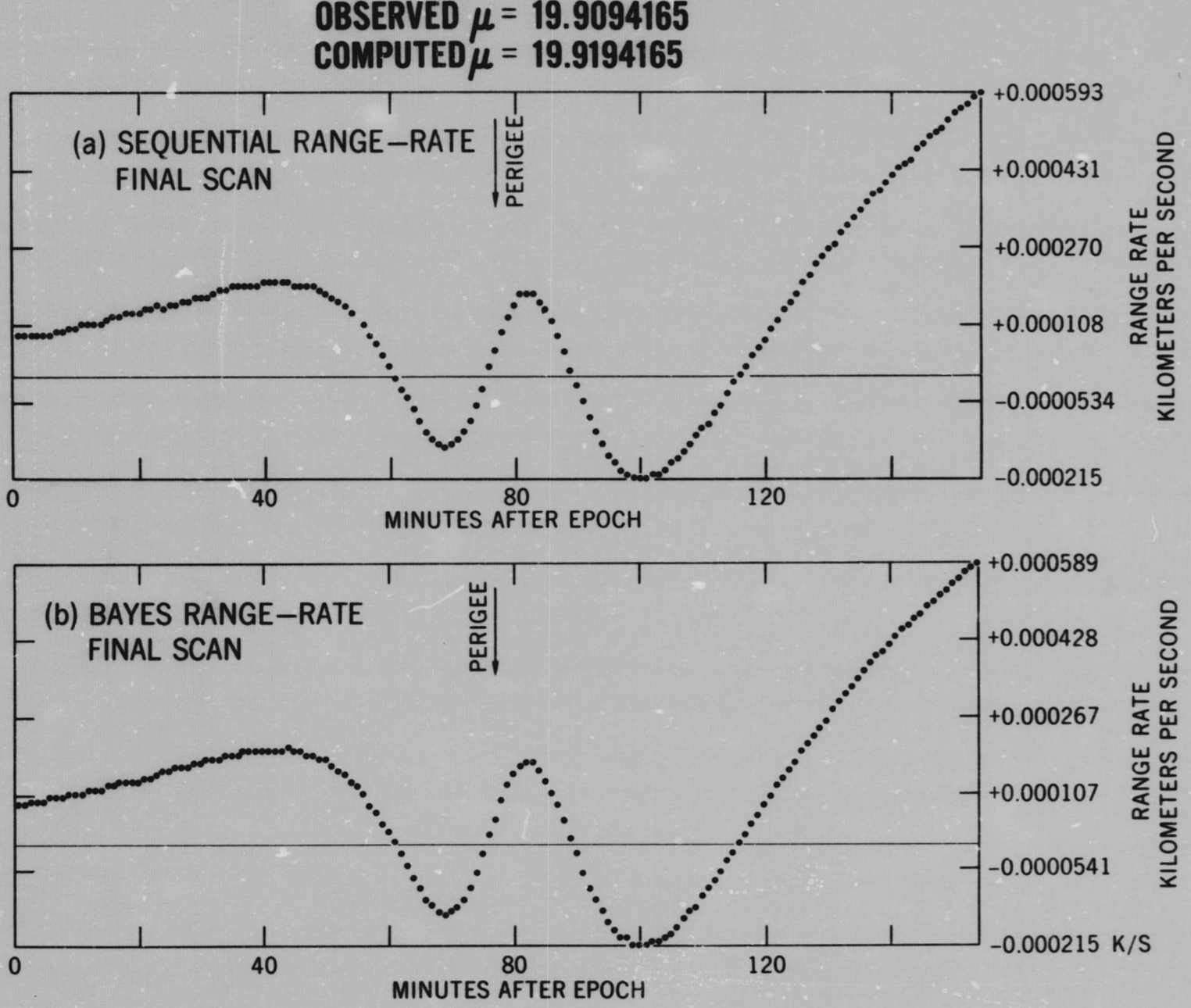
BAYES-SEQUENTIAL EQUIVALENCE
RANGE AND RANGE-RATE OBSERVATIONS
OBSERVED μ = 19.9094165
COMPUTED μ = 19.9194165
(a) SEQUENTIAL RANGE–RATE
FINAL SCAN
PERIGEE
+0.000593
+0.000431
+0.000270
+0.000108
-0.0000534
-0.000215
RANGE RATE
KILOMETERS PER SECOND
0
40
80
120
MINUTES AFTER EPOCH
(b) BAYES RANGE–RATE
FINAL SCAN
PERIGEE
+0.000589
+0.000428
+0.000267
+0.000107
-0.0000541
-0.000215 K/S
RANGE RATE
KILOMETERS PER SECOND
0
40
80
120
MINUTES AFTER EPOCH

Figure 6

MODEL ERROR EFFECT

What happens to the system when the error in the model is accounted for? You may recall that in a sequential processor the state correction is given by $\Delta\alpha = L\,\Delta y$ where $\Delta\alpha$ is the correction to the state, Δy is the residual, i.e. observed minus computed observation and L is the Kalman gain matrix. The usual notation of Schmidt has been left to apply to the cartesian state. The notation here is one step up the alphabet for the alpha state hence the L rather than K for the Kalman gain matrix. When the state consists only of the six parameters

$$L = QN'\,Y^{-1}$$

where N is the sensitivity of the observation to the state $\partial y/\partial\alpha$, Q the covariance matrix and

$$Y = NQN' + \epsilon^{-2}$$

where ϵ^{-2} is the white noise variance.

If now the state is augmented by μ_b we have $\begin{pmatrix} Q & C_\mu \\ C_\mu & \mu_b \end{pmatrix}$ for the augmented state covariance. By accounting for the error we mean computing the augmented covariance but not updating μ_b nor decrementing its covariance. This is the procedure given by Schmidt. The gain then becomes

$$L = (QN' + C_\mu F')\,Y^{-1}$$

$$Y = NQN' + F\mu_b F' + NC_\mu F' + FC_\mu 'N' + \epsilon^{-2}$$

where F is the sensitivity of the observation to the new state variable $\frac{\partial y}{\partial \mu}$

The next four figures show what happens to the sequential processor during orbit determination when the bias is included.

Figure 7 shows the range without the bias matrix in the upper curve when both observation types are used. The lower curve shows how it behaves when the bias is included. The divergence of course disappears and the orbit continues to follow the observations.

Figure 8 is the range-rate.

Figure 9 shows the patterns when only range data are used; Figure 10 when only range-rate data are used.

The Bayes processor does not yet have this capability, but with the agreement we have already obtained, we have no reason to suspect that it will not get the same results as those shown in the next four figures.

Figure 11 shows the final range scan when both range and range-rate data were used. Obviously, the orbit fits the latter part of the data for the span of the model validity.

Figure 12 is the range-rate data for the same case.

Figure 13 shows what happens when range only is used and Figure 14 when range-rate is used by itself.

The advantage of using unsolved for biases should be apparent. The problem of modeling increases without limit as we proceed to higher and higher accuracies. Using unsolved for biases permits us to define a reasonable cutoff point at some finite accuracy and at some manageable computing complexity level. This point should vary depending on the purpose of the end product. Needless to say, prediction is always

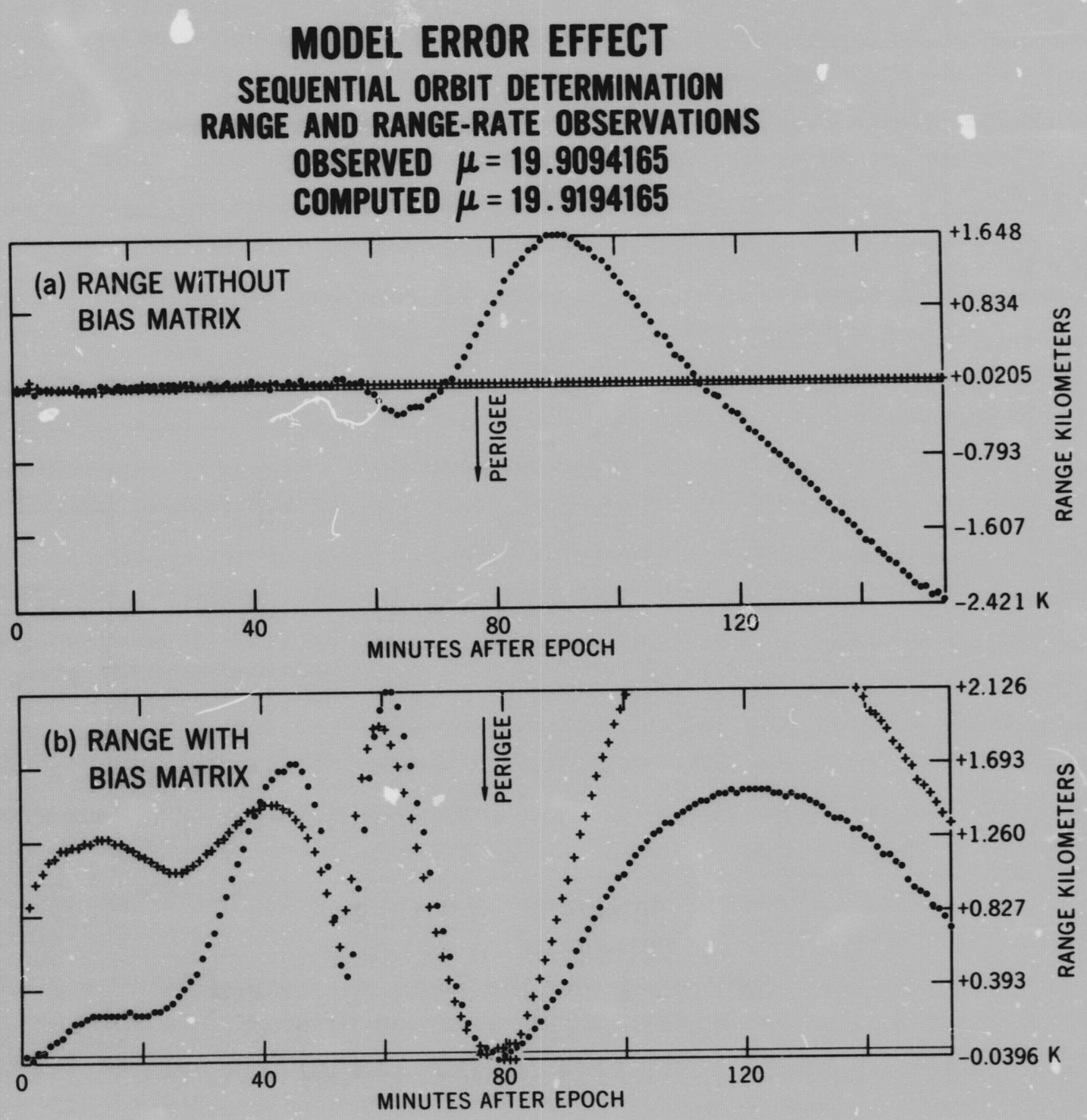
MODEL ERROR EFFECT
SEQUENTIAL ORBIT DETERMINATION
RANGE AND RANGE-RATE OBSERVATIONS
OBSERVED μ = 19.9094165
COMPUTED μ = 19.9194165
(a) RANGE WITHOUT BIAS MATRIX
PERIGEE
+1.648
+0.834
+0.0205
-0.793
-1.607
-2.421 K
RANGE KILOMETERS
0
40
80
120
MINUTES AFTER EPOCH
(b) RANGE WITH BIAS MATRIX
PERIGEE
+2.126
+1.693
+1.260
+0.827
+0.393
-0.0396 K
RANGE KILOMETERS
0
40
80
120
MINUTES AFTER EPOCH

Figure 7

MODEL ERROR EFFECT
SEQUENTIAL ORBIT DETERMINATION
RANGE AND RANGE-RATE OBSERVATIONS
OBSERVED μ= 19.9094165
COMPUTED μ= 19.9194165

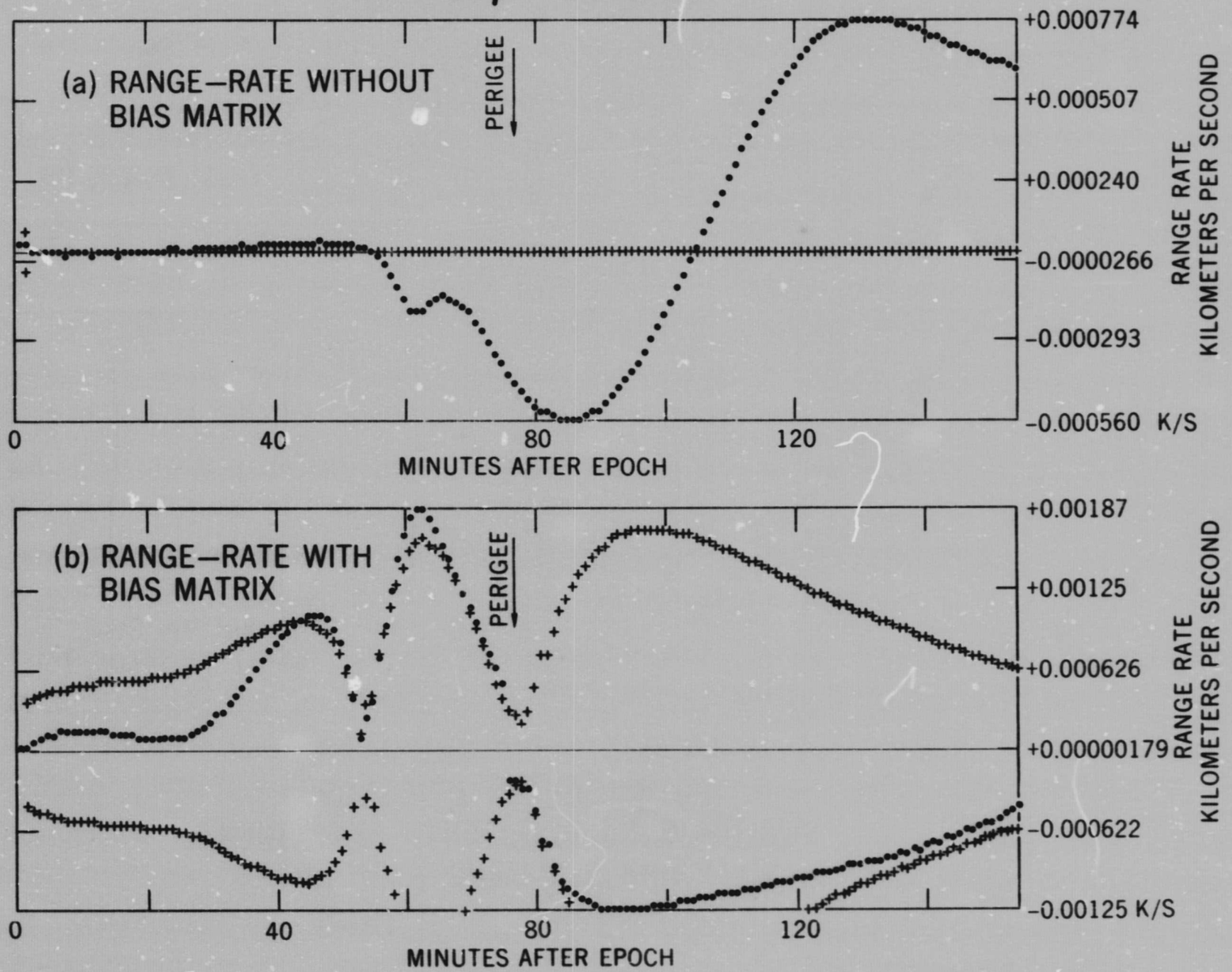

Figure 8

MODEL ERROR EFFECT
SEQUENTIAL ORBIT DETERMINATION
RANGE OBSERVATIONS
OBSERVED μ= 19.9094165
COMPUTED μ= 19.9194165
(a) RANGE WITHOUT BIAS MATRIX
PERIGEE
RANGE KILOMETERS
+0.215
+0.0914
-0.0319
-0.155
-0.278
-0.402 K
0
40
80
120
MINUTES AFTER EPOCH
(b) RANGE WITH BIAS MATRIX
PERIGEE
RANGE KILOMETERS
+1.16
+0.739
+0.322
-0.0955
-0.513
-0.930 K
0
40
80
120
MINUTES AFTER EPOCH

Figure 9

MODEL ERROR EFFECT
SEQUENTIAL ORBIT DETERMINATION
RANGE-RATE OBSERVATIONS
OBSERVED μ = 19.9094165
COMPUTED μ = 19.9194165
(a) RANGE–RATE WITHOUT BIAS MATRIX
PERIGEE
RANGE RATE KILOMETERS PER SECOND
+0.0000974
+0.0000634
+0.0000293
-0.00000468
-0.0000387
-0.0000727 K/S
0
40
80
120
MINUTES AFTER EPOCH
(b) RANGE–RATE WITH BIAS MATRIX
PERIGEE
RANGE RATE KILOMETERS PER SECOND
+0.000595
+0.000393
+0.000191
-0.0000105
-0.000212
-0.000414 K/S
0
40
80
120
MINUTES AFTER EPOCH

Figure 10

MODEL ERROR EFFECT
SEQUENTIAL FINAL SCAN
RANGE AND RANGE-RATE OBSERVATIONS
OBSERVED μ =19.9094165
COMPUTED μ =19.9194165

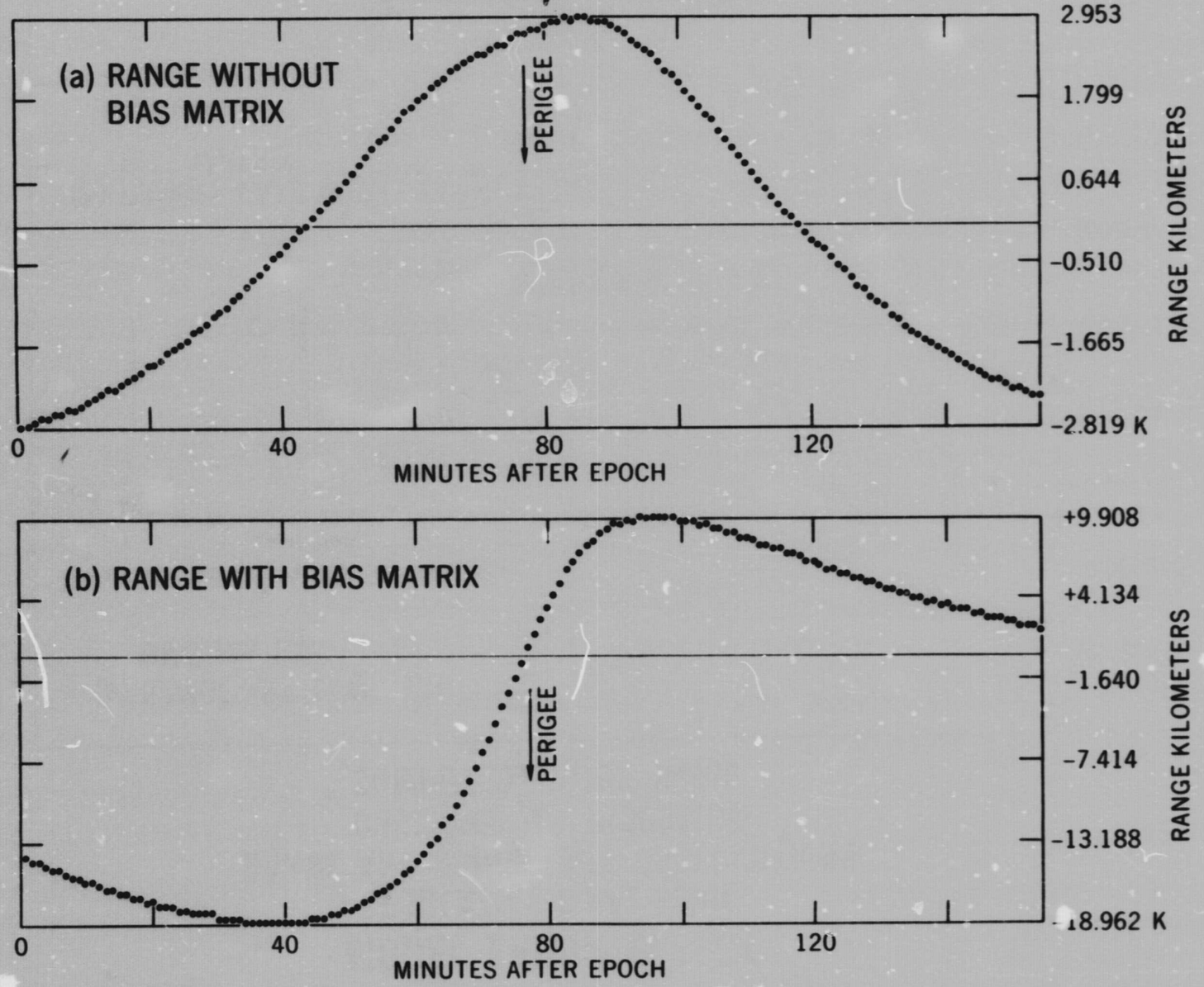

Figure 11

MODEL ERROR EFFECT
SEQUENTIAL FINAL SCAN
RANGE AND RANGE-RATE OBSERVATIONS
OBSERVED μ = 19.9094165
COMPUTED μ = 19.9194165
(a) RANGE–RATE WITHOUT BIAS MATRIX
PERIGEE
RANGE RATE KILOMETERS PER SECOND
+0.000593
+0.000431
+0.000270
+0.000108
-0.0000534
-0.000215 K/S
0
40
80
120
MINUTES AFTER EPOCH
(b) RANGE–RATE WITH BIAS MATRIX
PERIGEE
RANGE RATE KILOMETERS PER SECOND
+0.00944
+0.00718
+0.00492
+0.00266
+0.000406
-0.00185 K/S
0
40
80
120
MINUTES AFTER EPOCH

Figure 12

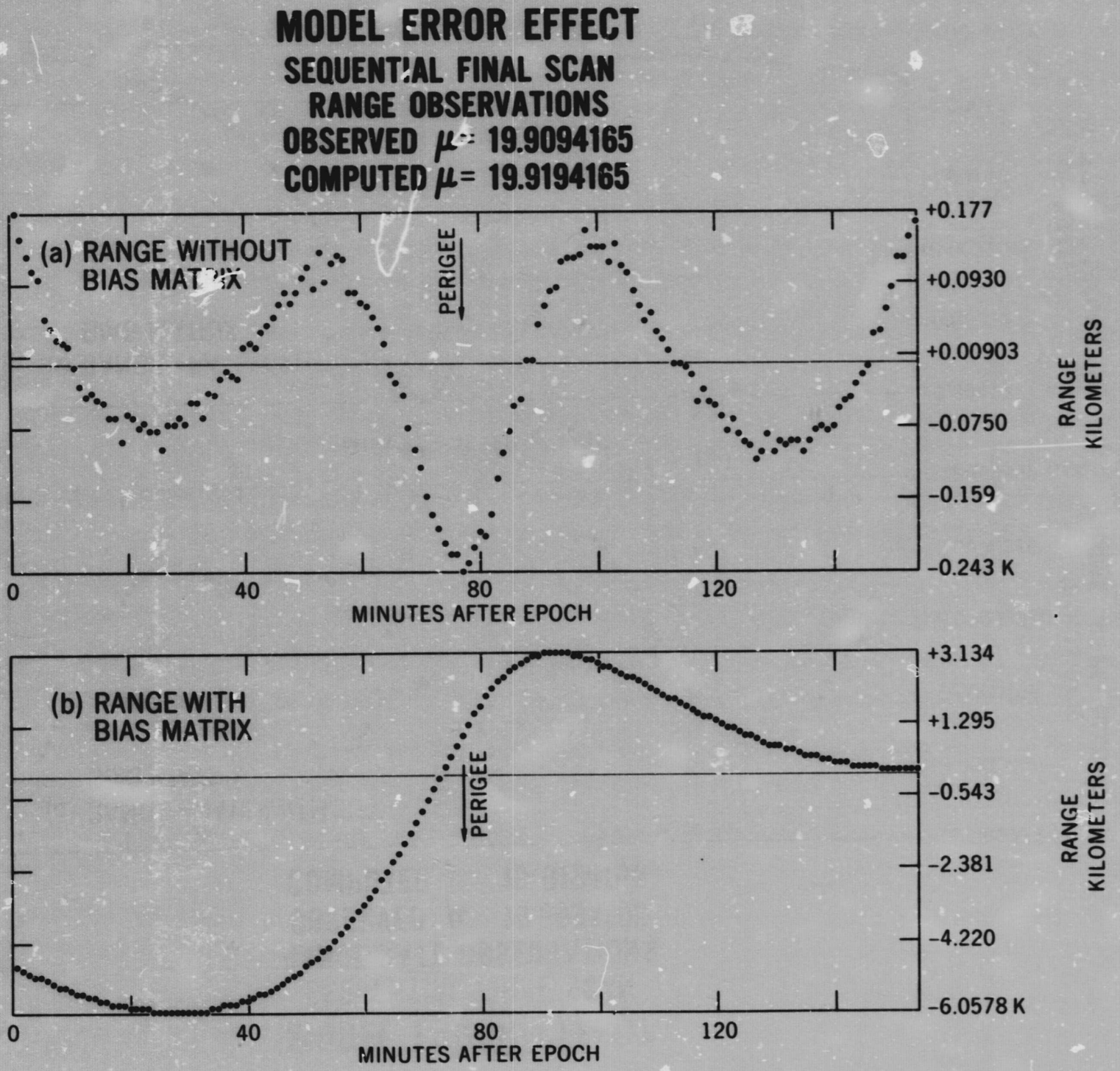
MODEL ERROR EFFECT
SEQUENTIAL FINAL SCAN
RANGE OBSERVATIONS
OBSERVED μ= 19.9094165
COMPUTED μ= 19.9194165
(a) RANGE WITHOUT BIAS MATRIX
PERIGEE
+0.177
+0.0930
+0.00903
-0.0750
-0.159
-0.243 K
RANGE KILOMETERS
0
40
80
120
MINUTES AFTER EPOCH
(b) RANGE WITH BIAS MATRIX
PERIGEE
+3.134
+1.295
-0.543
-2.381
-4.220
-6.0578 K
RANGE KILOMETERS
0
40
80
120
MINUTES AFTER EPOCH

Figure 13

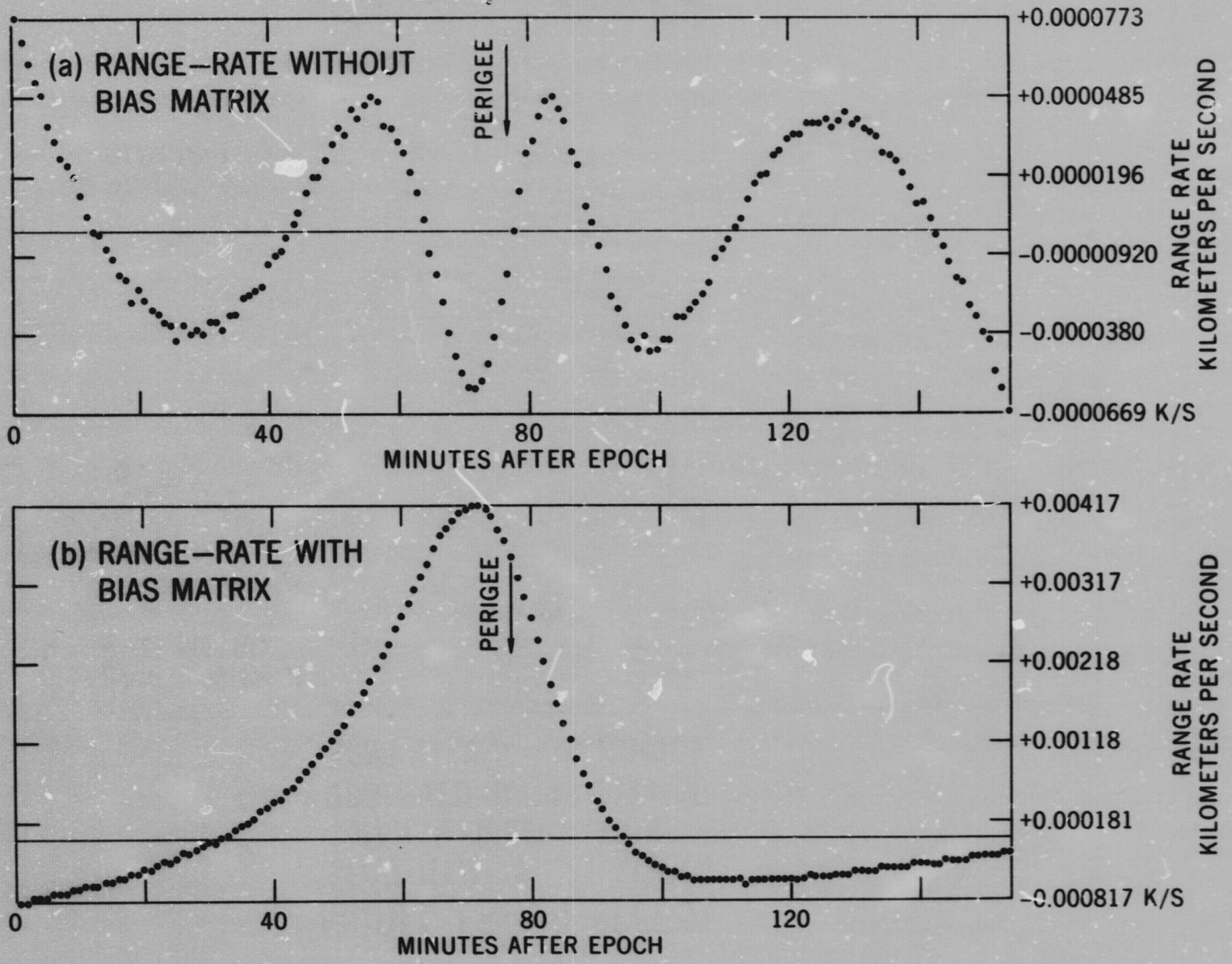
MODEL ERROR EFFECT
SEQUENTIAL FINAL SCAN
RANGE-RATE OBSERVATIONS
OBSERVED μ = 19.9094165
COMPUTED μ = 19.9194165
(a) RANGE–RATE WITHOUT BIAS MATRIX
PERIGEE
+0.0000773
+0.0000485
+0.0000196
-0.00000920
-0.0000380
-0.0000669 K/S
RANGE RATE KILOMETERS PER SECOND
0
40
80
120
MINUTES AFTER EPOCH
(b) RANGE–RATE WITH BIAS MATRIX
PERIGEE
+0.00417
+0.00317
+0.00218
+0.00118
+0.000181
-0.000817 K/S
RANGE RATE KILOMETERS PER SECOND
0
40
80
120
MINUTES AFTER EPOCH

Figure 14

model limited, therefore, prediction needs will dictate the required model accuracy. Beyond that the model should be cutoff with unsolved for biases. Only through this type of process can observations and orbit determination systems be utilized to their maximum efficiency.

RESIDUAL FREQUENCIES

The appearance of the final scan residuals led us to providing a preliminary scan capability in the program in order that we may study the complete evolution of the orbit determination process.

Figure 15 shows the comparison of preliminary and final scan for the range only observation case. It is clear, that the orbit determination process has introduced some spurious frequencies in the final residual pattern which could easily be mistaken for an error in $J_{2,0}$ or $J_{4,0}$ or some other coefficient rather than the central mass. We have suspected this for a long time but now there can be no doubt. In Figure 16 we see the same misfortune befalling the range-rate. It is at present only conjecture but we are quite confident that if we enlarge the state the situation will be far worse.

There is some hope for this dilemma as we shall see in the next two figures when range and range-rate observations are used. Figure 17 shows the range. Now the residual pattern is more like the error source that produced it, at least in the number of wave lengths and Figure 18 agrees showing the range-rate. This is a strong case for at least two and possibly more independent data types. It also explains to some extent why different data types find different orbits. Finally, it warns us to be cautious in the analysis of frequency content of residual

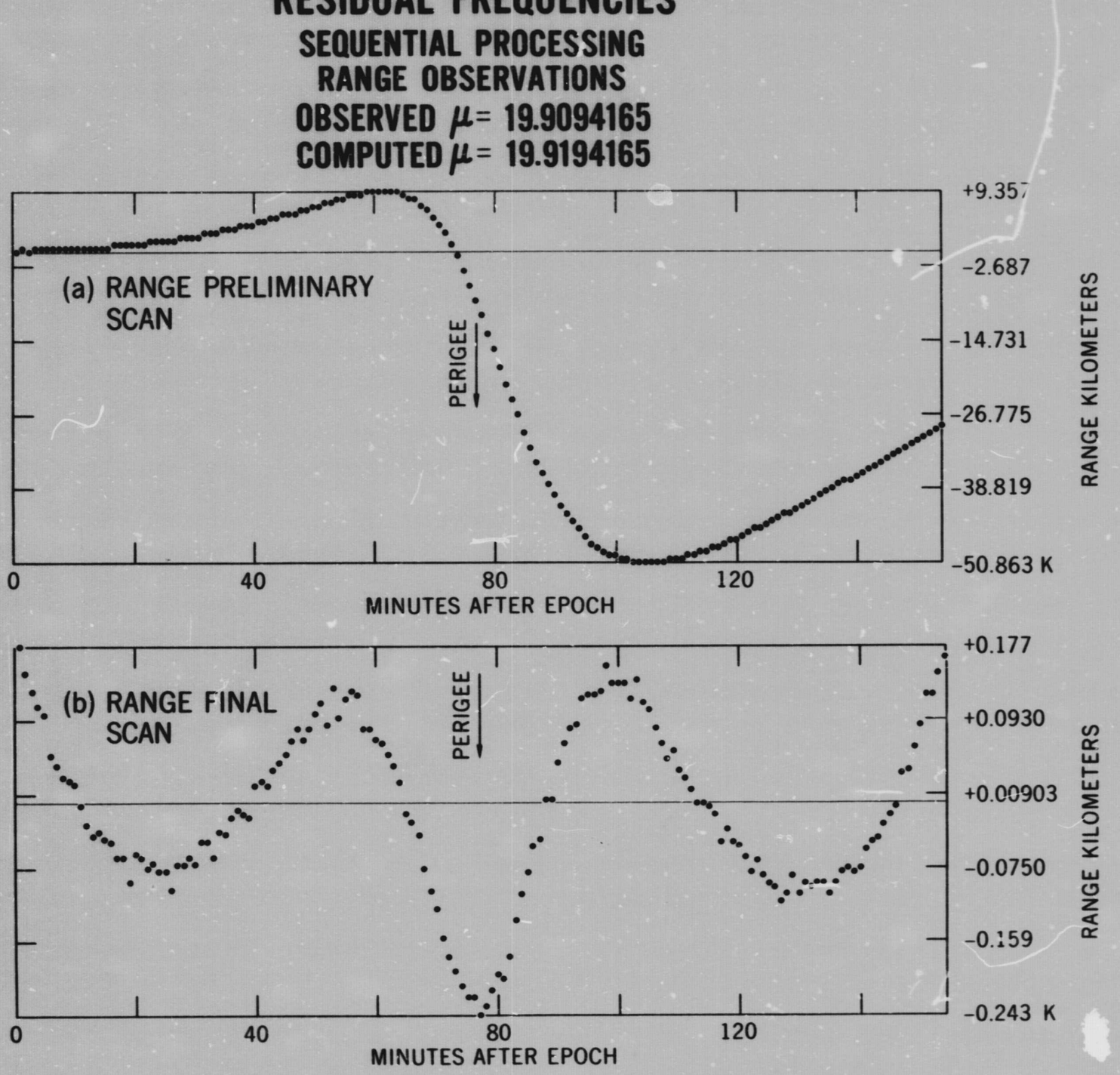
RESIDUAL FREQUENCIES
SEQUENTIAL PROCESSING
RANGE OBSERVATIONS
OBSERVED μ= 19.9094165
COMPUTED μ= 19.9194165
(a) RANGE PRELIMINARY SCAN
PERIGEE
+9.357
-2.687
-14.731
-26.775
-38.819
-50.863 K
RANGE KILOMETERS
0
40
80
120
MINUTES AFTER EPOCH
(b) RANGE FINAL SCAN
PERIGEE
+0.177
+0.0930
+0.00903
-0.0750
-0.159
-0.243 K
RANGE KILOMETERS
0
40
80
120
MINUTES AFTER EPOCH

Figure 15

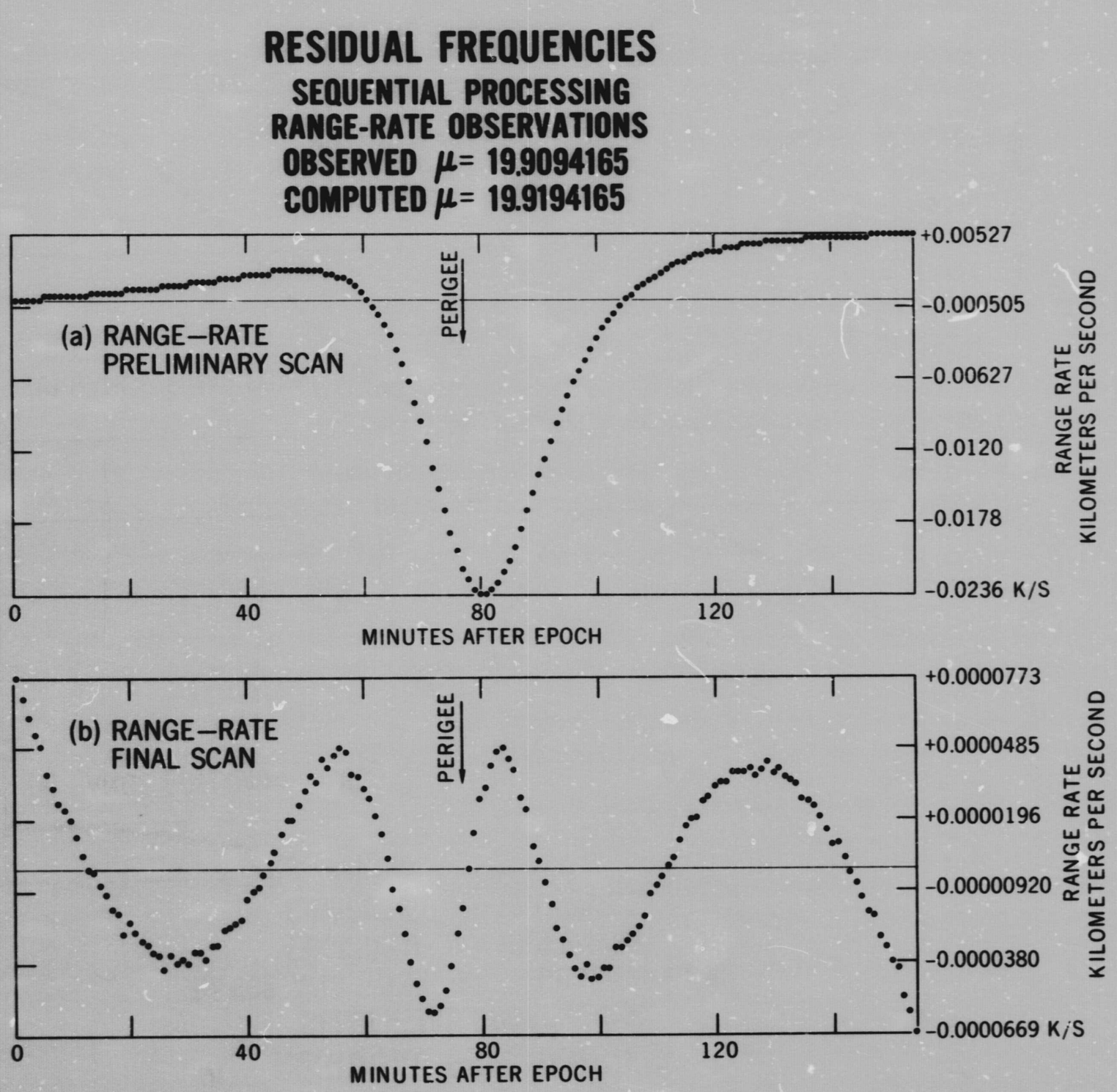
RESIDUAL FREQUENCIES
SEQUENTIAL PROCESSING
RANGE-RATE OBSERVATIONS
OBSERVED μ= 19.9094165
COMPUTED μ= 19.9194165
(a) RANGE–RATE
PRELIMINARY SCAN
PERIGEE
+0.00527
-0.000505
-0.00627
-0.0120
-0.0178
-0.0236 K/S
RANGE RATE
KILOMETERS PER SECOND
0
40
80
120
MINUTES AFTER EPOCH
(b) RANGE–RATE
FINAL SCAN
PERIGEE
+0.0000773
+0.0000485
+0.0000196
-0.00000920
-0.0000380
-0.0000669 K/S
RANGE RATE
KILOMETERS PER SECOND
0
40
80
120
MINUTES AFTER EPOCH

Figure 16

RESIDUAL FREQUENCIES
SEQUENTIAL PROCESSING
RANGE AND RANGE-RATE OBSERVATIONS
OBSERVED μ = 19.9094165
COMPUTED μ = 19.9194165

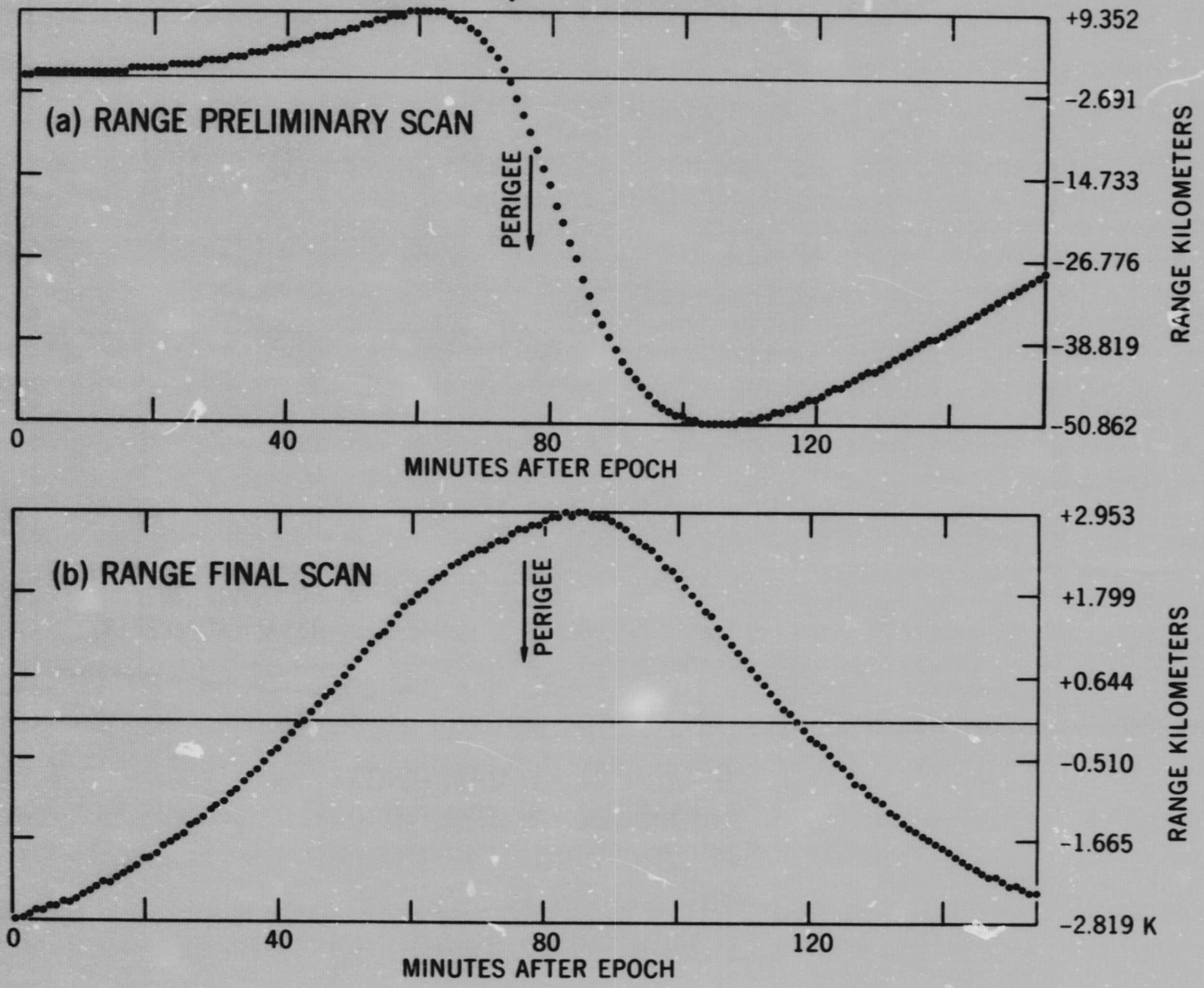

Figure 17

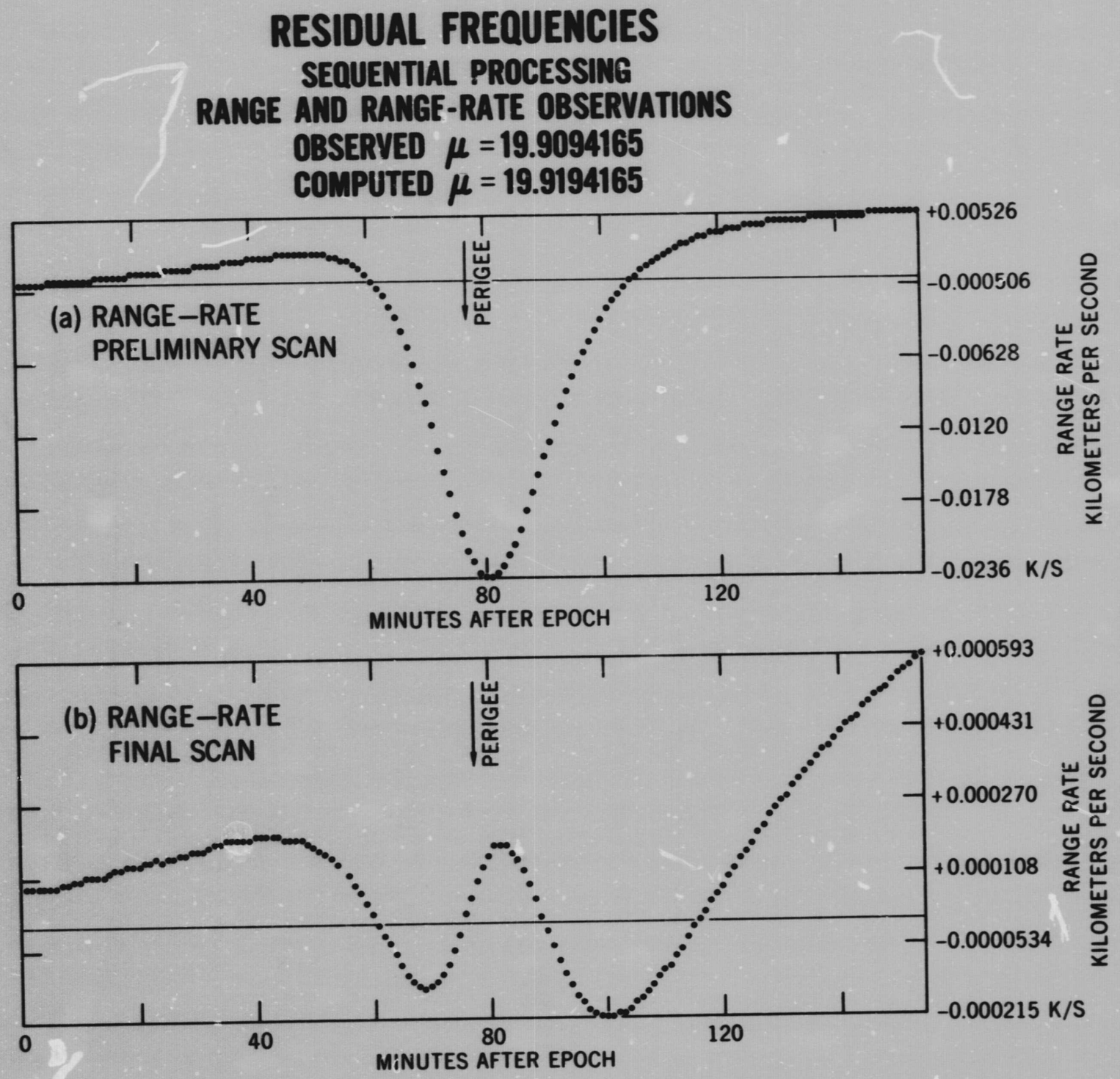
RESIDUAL FREQUENCIES
SEQUENTIAL PROCESSING
RANGE AND RANGE-RATE OBSERVATIONS
OBSERVED μ = 19.9094165
COMPUTED μ = 19.9194165
(a) RANGE–RATE
PRELIMINARY SCAN
PERIGEE
+0.00526
-0.000506
-0.00628
-0.0120
-0.0178
-0.0236 K/S
RANGE RATE
KILOMETERS PER SECOND
0
40
80
120
MINUTES AFTER EPOCH
(b) RANGE–RATE
FINAL SCAN
PERIGEE
+0.000593
+0.000431
+0.000270
+0.000108
-0.0000534
-0.000215 K/S
RANGE RATE
KILOMETERS PER SECOND
0
40
80
120
MINUTES AFTER EPOCH

Figure 18

patterns when a single observation type is used or dominates the determination, i.e. far greater accuracy than any others.

Having obtained these results and noting the lunar orbiter difficulties we decided to simulate with the earth, a crude approximation to the mascon processing.

In Figure 19, we see the residual pattern for range, when both range and range-rate were used as observations. In all of this series we used the same data as before but now, the error we have imposed is the use of a spherical earth for the orbit determination.

In Figure 20 the range-rate residuals are shown--nothing alarming in either of these.

In Figure 21 we see what the residuals are like when range only is used and now strange things are happening.

In Figure 22 we see a very familiar pattern when range-rate is used alone. Before you jump to the conclusion that this is a fault of sequential processing look at Figure 23 which compares sequential and Bayes with range-rate only. We should further say that all the runs, with the exception of the unsolved for bias have been verified using the Bayes.

In the final Figure 24, we further demonstrate the comparison by showing the lunar orbiter residuals and ours on the same figure.

I do not have the figure, but I can say that divergence occurred prior to reaching perigee in the determination pass.

We have of course only demonstrated a striking similarity on a single pass but we feel it certainly warrants further investigation. We offer no explanation for the high correlation of Mascons with surface

RESIDUAL PATTERNS
SEQUENTIAL PROCESSING
RANGE AND RANGE-RATE OBSERVATIONS
OBSERVED SAO '66
COMPUTED SPHERICAL EARTH

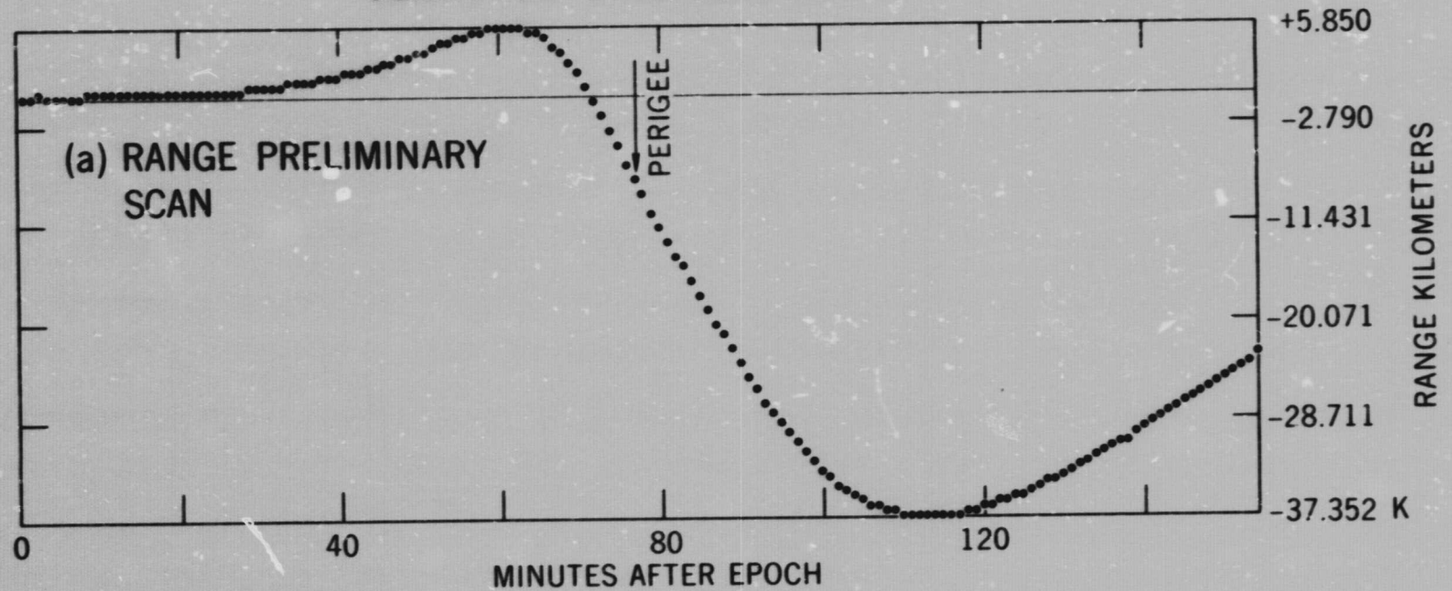

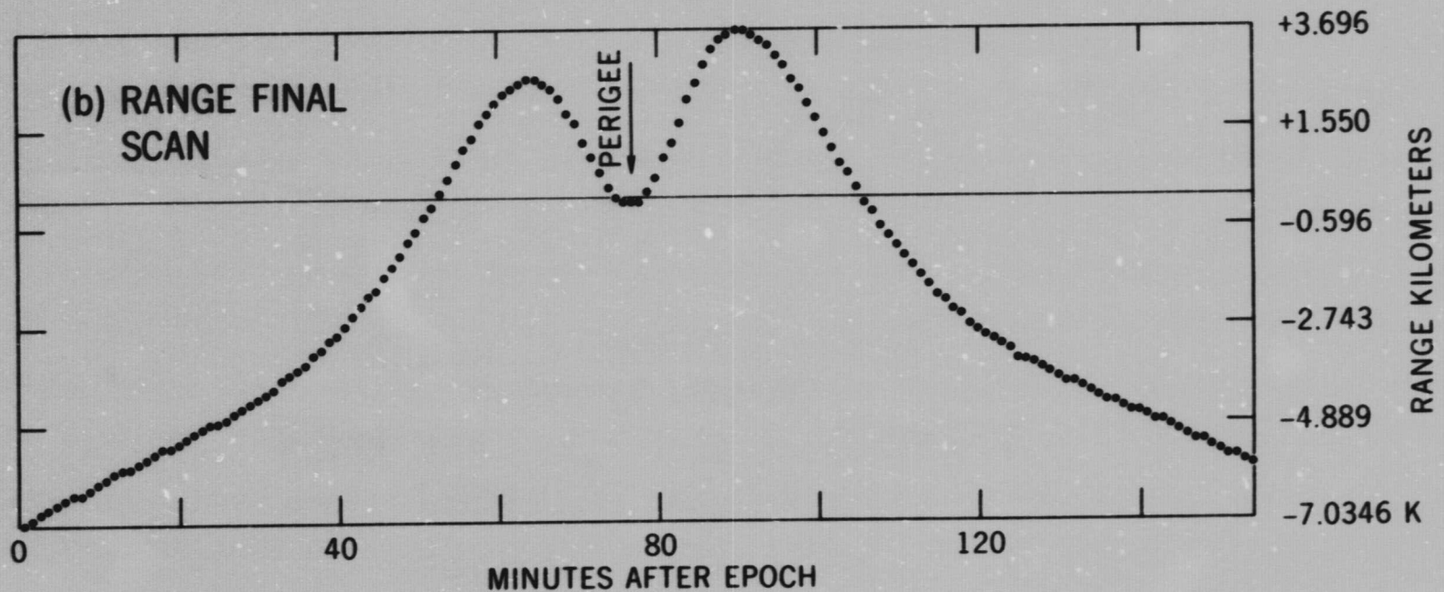

Figure 19

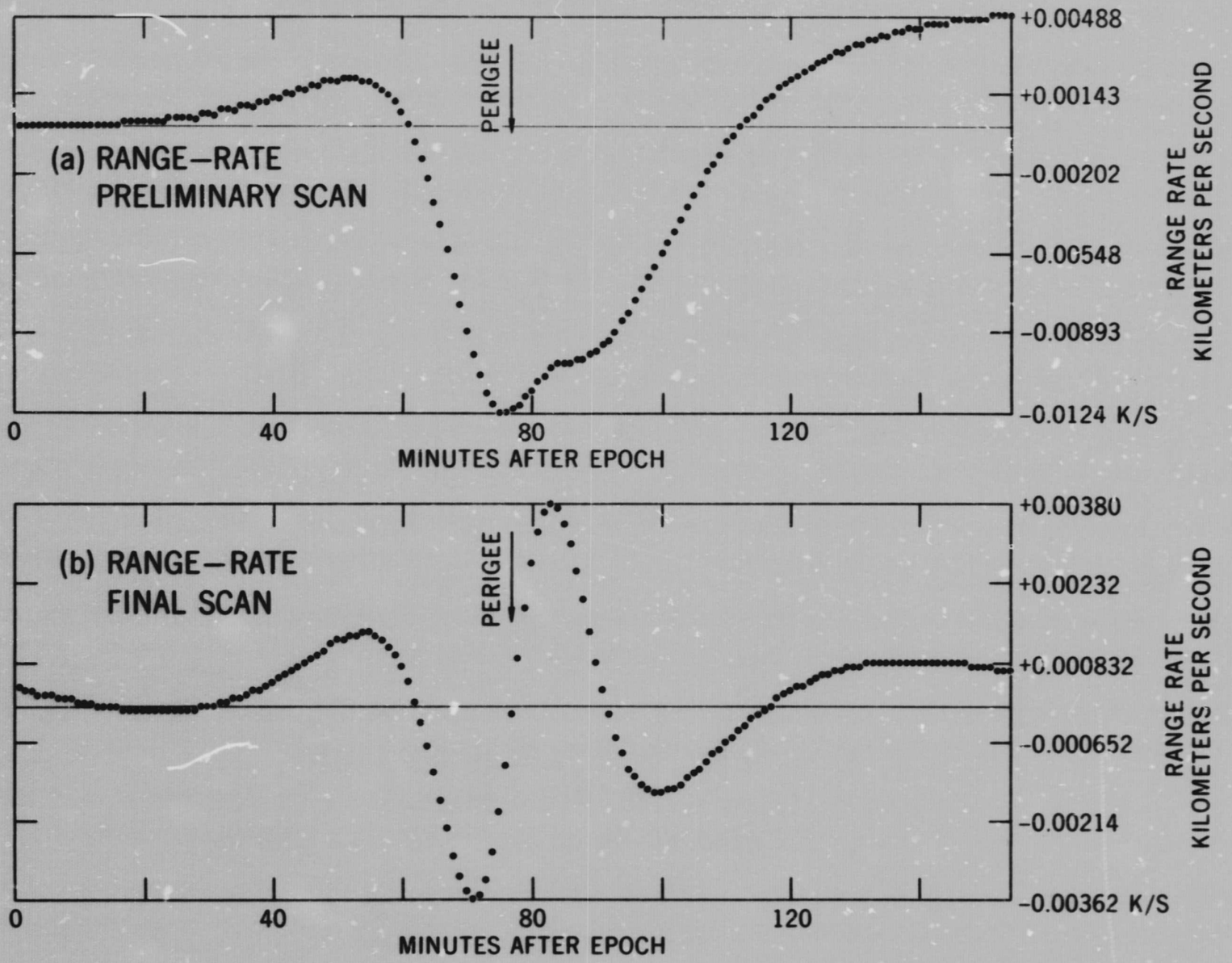
RESIDUAL PATTERNS
SEQUENTIAL PROCESSING
RANGE AND RANGE-RATE OBSERVATIONS
OBSERVED SAO '66
COMPUTED SPHERICAL EARTH
(a) RANGE–RATE
PRELIMINARY SCAN
PERIGEE
+0.00488
+0.00143
-0.00202
-0.00548
-0.00893
-0.0124 K/S
RANGE RATE
KILOMETERS PER SECOND
0
40
80
120
MINUTES AFTER EPOCH
(b) RANGE–RATE
FINAL SCAN
PERIGEE
+0.00380
+0.00232
+0.000832
-0.000652
-0.00214
-0.00362 K/S
RANGE RATE
KILOMETERS PER SECOND
0
40
80
120
MINUTES AFTER EPOCH

Figure 20

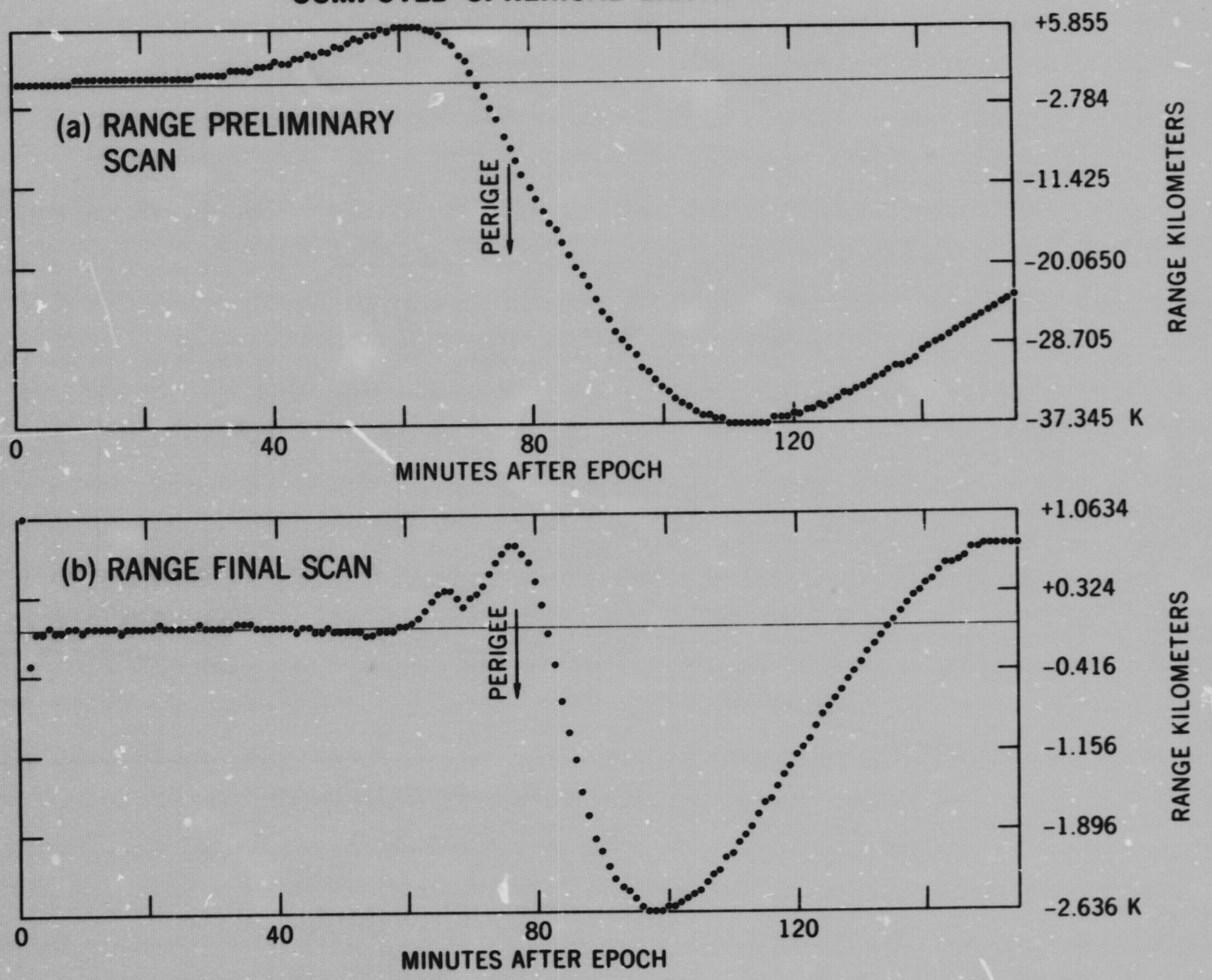
RESIDUAL PATTERNS
SEQUENTIAL PROCESSING
RANGE OBSERVATIONS
OBSERVED SAO '66
COMPUTED SPHERICAL EARTH
(a) RANGE PRELIMINARY SCAN
PERIGEE
+5.855
-2.784
-11.425
-20.0650
-28.705
-37.345 K
RANGE KILOMETERS
0
40
80
120
MINUTES AFTER EPOCH
(b) RANGE FINAL SCAN
PERIGEE
+1.0634
+0.324
-0.416
-1.156
-1.896
-2.636 K
RANGE KILOMETERS
0
40
80
120
MINUTES AFTER EPOCH

Figure 21

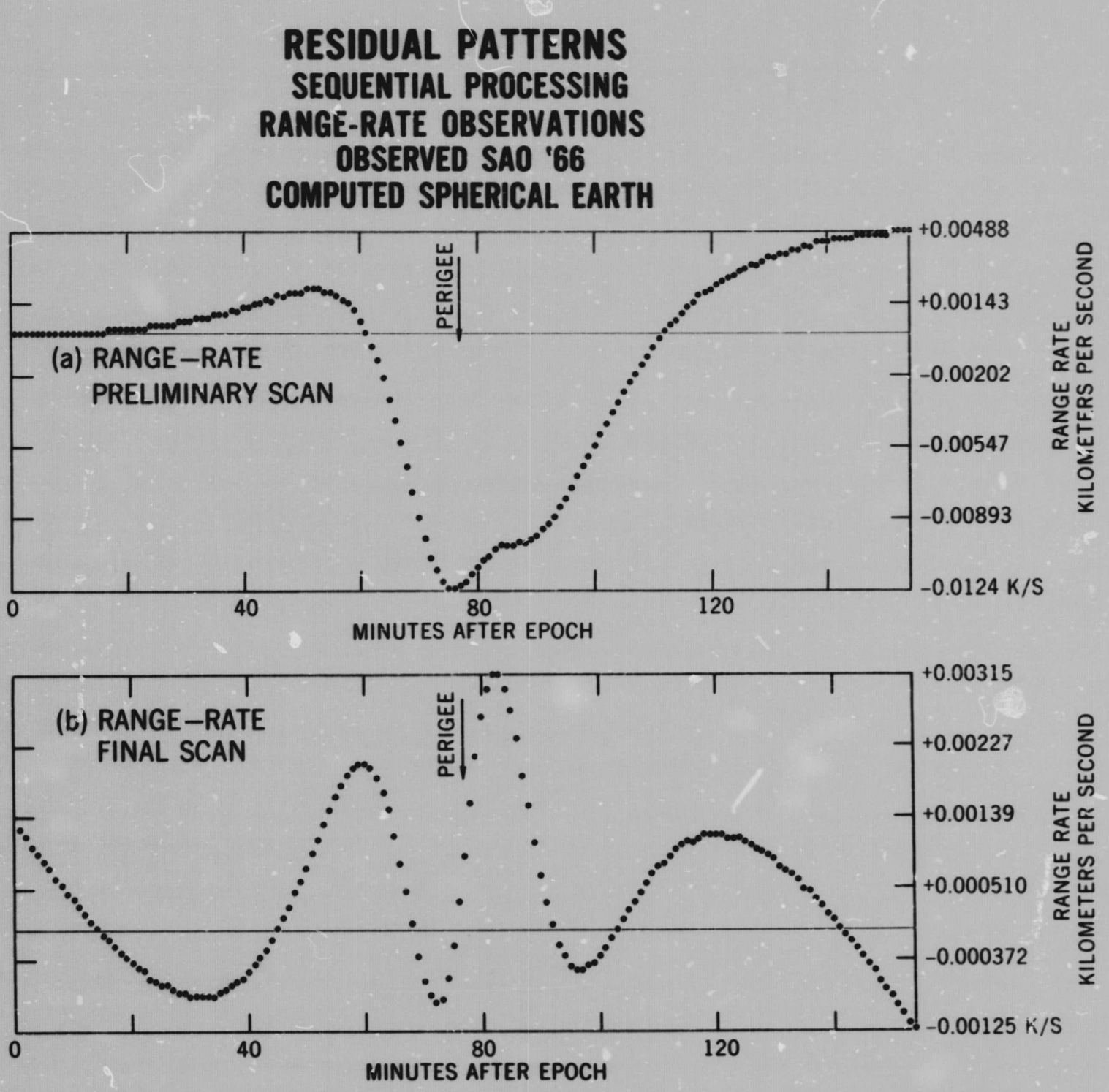
RESIDUAL PATTERNS
SEQUENTIAL PROCESSING
RANGE-RATE OBSERVATIONS
OBSERVED SAO '66
COMPUTED SPHERICAL EARTH
(a) RANGE–RATE
PRELIMINARY SCAN
PERIGEE
+0.00488
+0.00143
-0.00202
-0.00547
-0.00893
-0.0124 K/S
RANGE RATE
KILOMETERS PER SECOND
0
40
80
120
MINUTES AFTER EPOCH
(b) RANGE–RATE
FINAL SCAN
PERIGEE
+0.00315
+0.00227
+0.00139
+0.000510
-0.000372
-0.00125 K/S
RANGE RATE
KILOMETERS PER SECOND
0
40
80
120
MINUTES AFTER EPOCH

Figure 22

RESIDUAL PATTERNS
RANGE-RATE OBSERVATIONS
OBSERVED SAO '66
COMPUTED SPHERICAL EARTH
(a) SEQUENTIAL FINAL SCAN
PERIGEE
RANGE RATE
KILOMETERS PER SECOND
+0.00315
+0.00227
+0.00139
+0.000510
-0.000372
-0.00125 K/S
0
40
80
120
MINUTES AFTER EPOCH
(b) BAYES FINAL SCAN
PERIGEE
RANGE RATE
KILOMETERS PER SECOND
+0.00214
+0.00136
+0.000577
-0.000206
-0.000990
-0.00177 K/S
0
40
80
120
MINUTES AFTER EPOCH

Figure 23

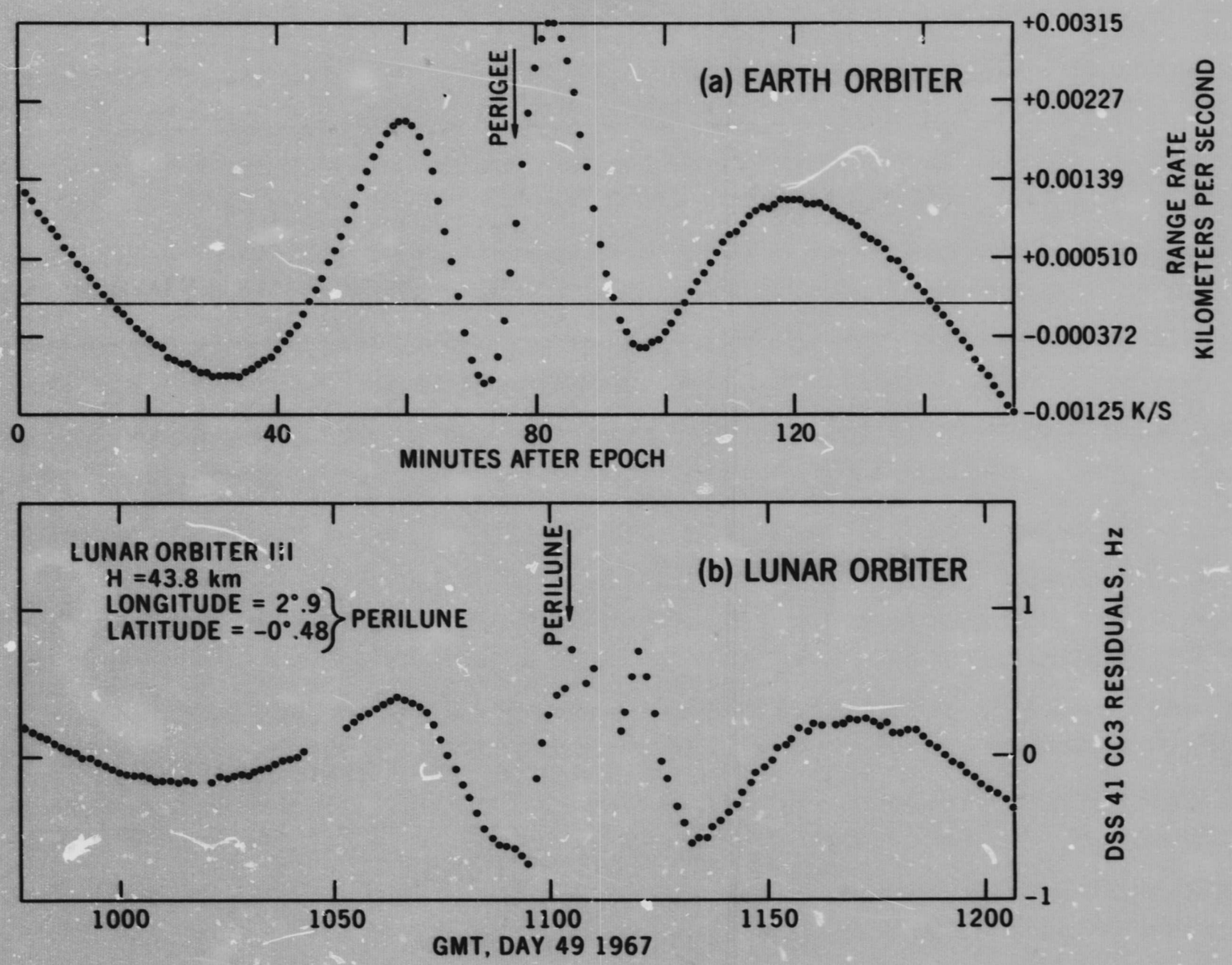
A. COMPARISON
(a) EARTH ORBITER
PERIGEE
+0.00315
+0.00227
+0.00139
+0.000510
-0.000372
-0.00125 K/S
RANGE RATE
KILOMETERS PER SECOND
0
40
80
120
MINUTES AFTER EPOCH
LUNAR ORBITER III
H =43.8 km
LONGITUDE = 2°.9
LATITUDE = -0°.48
PERILUNE
PERILUNE
(b) LUNAR ORBITER
1
0
-1
DSS 41 CC3 RESIDUALS, Hz
1000
1050
1100
1150
1200
GMT, DAY 49 1967

Figure 24

features we prefer to leave that to the Mascon investigators.

In conclusion, we think we have begun a very enlightening study for those of us in the orbit determination business. This was begun as a prelude to the acquisition of continuous tracking of earth satellites from orbiting tracking stations. However, as complex as orbit determination models are, there is a large amount of room for other investigators to follow analogous research and we would like to encourage as many of you as possible to do so. Our programs though not designed for export, are available in as is condition.

Our sequential processor has an error analysis mode which we have been using to check out error analysis programs. Let it suffice to say, that there should be a requirement placed on all vendors of error analysis programs to include the generation of observations and differential correction in order to verify that it is properly including the effect of each error source. There is no better method of checking such a program. Test cases should include a separate one for each error source and all combinations and permutations thereof.